



Indian Journal of Engineering

Frictional and Constant Temperature Heating Control of Air Flow in Diverging Part of Horizontal Nozzles

Samheri A.R. Almuradi

Ph.D. Lecturer, General Supervisor of Postgraduate Lab., Mech. Eng. Dept., Faculty of Engineering, Al-Mustansiriya University, Baghdad, Iraq; P.O. Box (46049), Baghdad, Iraq. E-mail: samheri_a@yahoo.com; Mobile: 00964 7901182377

Publication History

Received: 25 September 2016

Accepted: 22 October 2016

Published: October-December 2016

Citation

Samheri AR Almuradi. Frictional and Constant Temperature Heating Control of Air Flow in Diverging Part of Horizontal Nozzles. *Indian Journal of Engineering*, 2016, 13(34), 680-697

Publication License



© The Author(s) 2016. Open Access. This article is licensed under a [Creative Commons Attribution License 4.0 \(CC BY 4.0\)](https://creativecommons.org/licenses/by/4.0/).

General Note



Article is recommended to print as digital color version in recycled paper.

ABSTRACT

The study is concerned with the interference of friction in constant temperature heating inside the diverging part of a converging-diverging nozzle working at design condition where the velocity changes to supersonic flow regime from a Mach no. of 1.0. Set of gas-dynamic equations are completed using numerical approximation of the dimensionless derivatives. A finite difference technique with 20% under – relaxation factor is applied. Most of these equations are non-linear along from the throat till the nozzle exit with a wide range of frictional forces from 0.001 to 0.003 average frictional factor ranges with 0.00025 steps. The results are distributed

Samheri,
Frictional and Constant Temperature Heating Control of Air Flow in Diverging Part of Horizontal Nozzles,
Indian Journal of Engineering, 2016, 13(34), 680-697,

between 3.0 and 4.0 area ratio of non-linear inside nozzle curvature. The multi mixing of all variables help to give results different and more accurate values than isentropic or with isothermal or frictional states or with double mixing of any of them to be more close to experimental ones. These all together have been considered in our model which has employed all variables which will assist in the optimum design for real type of nozzles.

Keywords: frictional, constant temperature heating, Supersonic air flow, diverging part of nozzle.

NOMENCLATURE

A	Cross-sectional-area in m^2
A_e	Exit cross-sectional area in m^2
A^*	Critical cross-sectional area in m^2
a, b & c	Area shape constants
DR	Mass density Ratio ($\frac{\rho}{\rho^*}$)
ρ	Mass density in $kg-m^{-3}$
ρ^*	Critical mass density in $kg-m^{-3}$
v	Flow velocity in $m-s^{-1}$
v^*	Critical velocity in $m-s^{-1}$
VR	Velocity ratio (v/v^*)
ER	Area-ratio (A/A^*)
ERE	Exit area-ratio (A_e/A^*)
\bar{f}	Average friction factor
F	Frictional force in N
k	Specific heat ratio
L	Real length of duct in m
m^0	Mass-flow-rate in $kg-s^{-1}$
M	Mach number
P	Pressure in kpa
P^*	Critical pressure in kpa
P_o	Stagnation pressure in kpa
P_o^*	Critical stagnation pressure in kpa
PR	Pressure ratio (P/P^*)
PZR	Stagnation pressure ratio (P_o/P_o^*)
r	Under relaxation factor
R	Gas-constant in $J-kg^{-1}-K^{-1}$
S	Entropy property in $J-kg^{-1}-K^{-1}$
S^*	Critical Entropy in $J-kg^{-1}-K^{-1}$
$S-S^*$	Entropy change in $J-kg^{-1}-K^{-1}$
$S-S^*/R$	Entropy change ratio
T	Temperature in K
T^*	Critical temperature in K
T_o	Stagnation temperature in K
T_o^*	Critical stagnation temperature in K
TR	Temperature ratio (T/T^*)
TZR	Stagnation temperature ratio (T_o/T_o^*)
x	Distance along nozzle in m
X	Dimensionless distance (x/L)

1. INTRODUCTION

Most of related studies about engines of aircrafts or space-shuttles or different kinds of rockets are concentrated on flows in supersonic regime of properties. The assembly of most variables take place will close the studies to a more reality, as long as the prediction is coming to exact points. This is very important in modern design condition of nozzles operation. Reference [15] has described the experimental study of a supersonic interval flow through a converging –diverging nozzle. The Mach no. distribution obtained using traversing of a pilot-Pitot –Tube. The used converging-diverging nozzle has an area-ratio of 2.867. Even the scope of their study was to investigate the improvement of flow using types of riblets, but the smooth surface tests can be compared with present study. Therefore their study lacks to theoretical analysis, mainly in the supersonic part between throat and nozzle exit. Since that study employed a draft wind tunnel, however can be stated as a constant temperature (isothermal) type tests. Also smooth surface tests [15] assumed a coefficient of friction of 0.0028 in their tests. They examined the distribution of both the static and dynamic pressures.

Reference [4], has verified and validated of the quasi-one dimensional pressure based on finite volume algorithm, implemented in Generalized Fluid System Simulation Program (GFSSP), for predicting compressible flow with friction, heat transfer and area change. Their converging-diverging nozzle configuration area ratio was 4.0 with an internal wall average friction factor of 0.002. They concentrated on the chocking condition of nozzle mode of operation, i.e. subsonic flow regime within the diverging part of nozzle after chocking ($M = 1.0$) at around throat due to all friction, heat transfer and area. So they left the supersonic mode of operation (design condition).

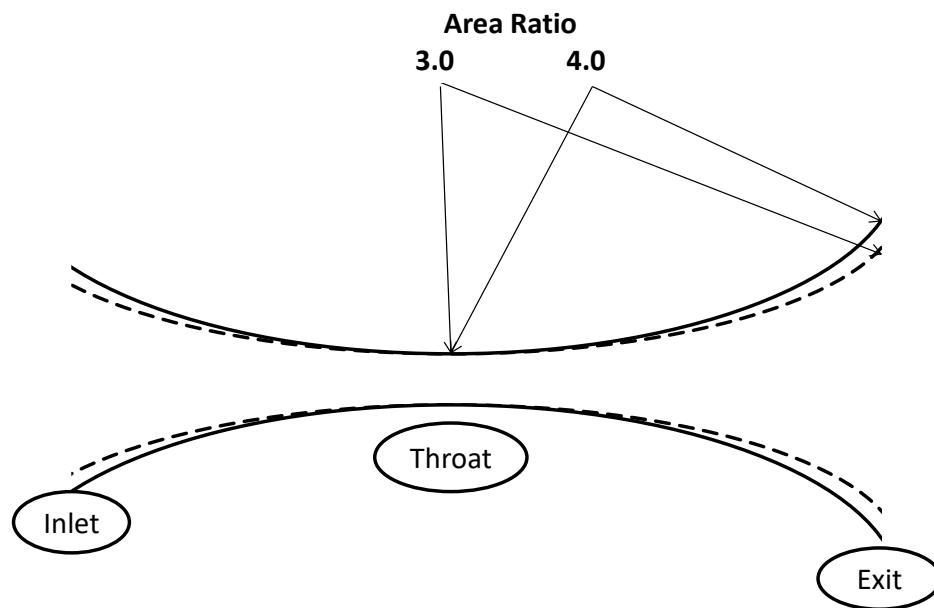


Figure 1 Schematic of a converging-diverging nozzle.

As well known the inside wall of variable area duct will subject to friction in spite the lower distance along the duct in addition to isothermal or heat-transfer induced together. The one of preferred methods to analyze the compressible fluid flow regimes are numerical methods. The real power of the numerical approach is, however, felt when problems for which it is difficult to obtain analytical solutions are considered. The methods used to analyze one variable separately. Studies on area-variation or friction or isothermal are proceeded before in constant area ducts or a mix between two of them. In the present study the analysis with full effect of the three types of flows will employed here using a finite-difference numerical model after experiencing it to be more applicable with such complex algorithm forms. At the same time a comparison is made with two flow types solved with the same

numerical method. Not only this but also examine different real frictional forces in addition to real two area ratio configurations and analyze all flow properties in addition to Entropy change, as shown in figure (1). The numerical model deals with the supersonic flow regime in the design operation mode condition. The analysis is difficult to employ using normal analytical solutions.

2. AREA VARIATION FLOW MODEL

The conservation of mass between any static and critical states in an isentropic area variation model are [1], [7], [11], [16] and [17],

$$\dot{m} = \rho \cdot v \cdot A = \rho^* \cdot v^* \cdot A^* \quad \dots (1)$$

$$\frac{\rho}{\rho^*} = \frac{v^* \cdot A^*}{v \cdot A} \quad \dots (2)$$

Conservation of momentum between same states before is,

$$F + P^* \cdot A^* - P \cdot A = \dot{m}(v - v^*) \quad \dots (3)$$

The fluid force is,

$$F = \left(P^* + \frac{P - P^*}{2} \right) (A - A^*) \quad \dots (4)$$

Equation (3) becomes,

$$\left(P^* + \frac{P - P^*}{2} \right) (A - A^*) + P^* \cdot A^* - P \cdot A = \rho \cdot v^2 \cdot A - \rho^* \cdot v^{*2} \cdot A^* \quad \dots (5)$$

$$\frac{1}{2} P^* \cdot A - \frac{1}{2} P \cdot A - \frac{1}{2} P \cdot A^* + \frac{1}{2} P^* \cdot A^* = \rho \cdot v^2 \cdot A - \rho^* \cdot v^{*2} \cdot A^* \quad \dots (6)$$

$$\frac{1}{2} A(P^* - P) + \frac{1}{2} A^*(P^* - P) = \rho \cdot v^2 \cdot A - \rho^* \cdot v^{*2} \cdot A^* \quad \dots (7)$$

$$\frac{1}{2} P^*(A + A^*) - \frac{1}{2} P(A + A^*) = \rho \cdot v^2 \cdot A - \rho^* \cdot v^{*2} \cdot A^* \quad \dots (8)$$

$$\frac{1}{2} P^*(A + A^*) + \left(\frac{P^*}{R \cdot T^*} \right) v^{*2} \cdot A^* = \frac{1}{2} P(A + A^*) + \left(\frac{P}{R \cdot T} \right) v^2 \cdot A \quad \dots (9)$$

Inserting Mach no. definition,

$$v = M \cdot \sqrt{k \cdot R \cdot T} \quad \dots (10)$$

$$P^* \left(\frac{A + A^*}{2} + k \cdot A^* \right) = P \left(\frac{A + A^*}{2} + M^2 \cdot k \cdot A \right) \quad \dots (11)$$

The non-dimensional pressure ratio will be,

$$\frac{P}{P^*} = \left(\frac{\frac{1}{2} \left(1 + \frac{A}{A^*} \right) + k}{\frac{1}{2} \left(1 + \frac{A}{A^*} \right) + k \cdot M^2} \right) \frac{A^*}{A} \quad \dots (12)$$

The relation of non-dimensional temperature ratio can get from the equation of state,

$$R = \frac{P}{\rho \cdot T} = \frac{P^*}{\rho^* \cdot T^*} \quad \dots (13)$$

$$\frac{T}{T^*} = \frac{P \cdot \rho^*}{P^* \cdot \rho} \quad \dots (14)$$

Substitute for (ρ^*/ρ) from equation (2),

$$\frac{T}{T^*} = \frac{P \cdot v \cdot A}{P^* \cdot v^* \cdot A^*} \quad \dots (15)$$

Again using the Mach no. definition,

$$\frac{T}{T^*} = \frac{P \cdot A \cdot M \sqrt{k \cdot R \cdot T}}{P^* \cdot A^* \sqrt{k \cdot R \cdot T^*}} \quad \dots (16)$$

$$\frac{T}{T^*} = \frac{(P \cdot A \cdot M)^2}{(P^* \cdot A^*)^2} \quad \dots (17)$$

Substitute for (P/P^*) from equation (12),

$$\frac{T}{T^*} = \frac{M^2 \left(\frac{1}{2} \left(1 + \frac{A}{A^*} \right) + k \right)^2}{\left(\frac{1}{2} \left(1 + \frac{A^*}{A} \right) + k \cdot M^2 \right)^2} \quad \dots (18)$$

The non-dimensional velocity ratio can be obtained from equation (15),

$$\frac{v}{v^*} = \frac{T}{T^*} \left(\frac{P^* \cdot A^*}{P \cdot A} \right) \quad \dots (19)$$

Substitute for non-dimensional temperature and pressure ratios from equations (12) and (18), respectively,

$$\frac{v}{v^*} = \frac{M^2 \left(\frac{1}{2} \left(1 + \frac{A}{A^*} \right) + k \right)}{\frac{1}{2} \left(1 + \frac{A^*}{A} \right) + k \cdot M^2} \quad \dots (20)$$

Using equations (2) and (20) to find the non-dimensional density ratio,

$$\frac{\rho}{\rho^*} = \frac{A^* \left(\frac{1}{2} \left(1 + \frac{A^*}{A} \right) + k \cdot M^2 \right)}{A \cdot M^2 \left(\frac{1}{2} \left(1 + \frac{A}{A^*} \right) + k \right)} \quad \dots (21)$$

Then applying the adiabatic law to find the non-dimensional stagnation temperature ratio,

$$\frac{T_o}{T_o^*} = \frac{T \left(1 + \frac{1}{2} (k-1) M^2 \right)}{T^* \left(1 + \frac{1}{2} (k-1) \right)} \quad \dots (22)$$

Again using equation (18),

$$\frac{T_o}{T_o^*} = \frac{M^2 \left(\frac{1}{2} \left(1 + \frac{A}{A^*} \right) + k \right)^2 \left(1 + \frac{1}{2} (k-1) M^2 \right)}{\left(\frac{1}{2} \left(1 + \frac{A^*}{A} \right) + k \cdot M^2 \right)^2 \left(1 + \frac{1}{2} (k-1) \right)} \quad \dots (23)$$

The stagnation pressure ratio can be obtained from,

$$\frac{P_o}{P_o^*} = \left(\frac{T_o}{T_o^*} \right)^{\frac{k}{k-1}} \quad \dots (24)$$

The non-dimensional Entropy change will be,

$$\frac{S - S^*}{R} = \frac{k}{k-1} \ln \frac{T}{T^*} - \ln \frac{P}{P^*} \quad \dots (25)$$

$$\frac{S - S^*}{R} = \ln \left[\frac{\left(\frac{T}{T^*} \right)^{\frac{k}{k-1}}}{\frac{P}{P^*}} \right] \quad \dots (26)$$

Substitute for (P/P^*) and (T/T^*) from equations (12) and (18), respectively,

$$\frac{S - S^*}{R} = \ln \left[\frac{M^2 \left(\frac{1}{2} \left(1 + \frac{A}{A^*} \right) + k \right)^{\frac{k}{k-1}}}{\left(\frac{1}{2} \left(1 + \frac{A}{A^*} \right) + k \right)^2} \right] - \ln \left[\frac{\left(\frac{A^*}{A} \right) \left(\frac{1}{2} \left(1 + \frac{A}{A^*} \right) + k \right)}{\frac{1}{2} \left(1 + \frac{A}{A^*} \right) + k \cdot M^2} \right] \quad \dots (27)$$

Note that the stagnation properties and Entropy are constant for isentropic flow only varied for other types of flow as will be shown.

3. DIMENSIONLESS FORMULATION

Continuity equation can be repeated using dimensionless values between initial state (1) and (i)th state as follows [11],

$$DR(i) = \frac{DR(1) \cdot VR(1) \cdot ER(1)}{VR(i) \cdot ER(i)} \quad \dots (28)$$

Pressure ratio in dimensional form is written as follows,

$$PR = \left(\frac{\frac{1}{2} (1 + ER) + k}{\frac{1}{2} \left(1 + \frac{1}{ER} \right) + k \cdot M^2} \right) \left(\frac{1}{ER} \right) \quad \dots (29)$$

The pressure ratio at state (1) is,

$$PR(1) = \left(\frac{\frac{1}{2} (1 + ER(1)) + k}{\frac{1}{2} \left(1 + \frac{1}{ER(1)} \right) + k \cdot M(1)^2} \right) \left(\frac{1}{ER(1)} \right) \quad \dots (30)$$

In the same manner the pressure ratio for (i)th state is,

$$PR(i) = \left(\frac{\frac{1}{2} (1 + ER(i)) + k}{\frac{1}{2} \left(1 + \frac{1}{ER(i)} \right) + k \cdot M(i)^2} \right) \left(\frac{1}{ER(i)} \right) \quad \dots (31)$$

Dividing equation (31) by equation (30),

$$PR(i) = PR(1) \left(\frac{\frac{1}{2} (1 + ER(i)) + k}{\frac{1}{2} (1 + ER(1)) + k} \right) \left(\frac{\frac{1}{2} \left(1 + \frac{1}{ER(1)} \right) + k \cdot M(1)^2}{\frac{1}{2} \left(1 + \frac{1}{ER(i)} \right) + k \cdot M(i)^2} \right) \left(\frac{ER(1)}{ER(i)} \right) \quad \dots (32)$$

Velocity ratio in dimensional form is written as follows,

$$k \cdot VR \cdot dVR = - \frac{dPR}{DR} \quad \dots (33)$$

Then make a backward property difference,

$$VR(i)(VR(i-1)) = - \left(\frac{1}{DR(i)} \right) \left(\frac{1}{k} \right) (PR(i) - PR(i-1)) \quad \dots (34)$$

$$VR(i) = VR(i-1) - \left(\frac{1}{k \cdot VR(i) \cdot DR(i)} \right) (PR(i) - PR(i-1)) \quad \dots (35)$$

4. NOZZLE SHAPE FORMULATION

The nozzle inside shape is such that the area variation with distance along the nozzle is best given by [11] in linear curvature, we modified the area equation to be used for non-linear curvature with higher degrees as required. Simply we formulate the following equation,

$$A(x) = a + bx + cx^2 \quad \dots (36)$$

The values of coefficients a, b and c in equation (36) in terms of the inlet (throat) and exit areas will first be determined,

When $x=0.0$ then $A=A^*$

When $x=L$ then $A=A_e$

When $x=0.0$ then $dA/dx=0.0$

Applying these conditions into area variation equation,

$$a=A^*, a+bL+cL^2=A_e, b=0.0$$

Equation (36) then becomes,

$$A = A^* + \frac{(A_e - A^*)x^2}{L^2} \quad \dots (37)$$

Now dividing equation (37) by A^* to get the non-dimensional form of area variation,

$$ER = 1 + (ERE - 1)X^2 \quad \dots (38)$$

5. NUMERICAL FORMULATION FOR AREA VARIATION MODEL

Because the equations governing fluid flow are non-linear, i.e. some of the terms in these equations involve products of flow variables; some form of iterative technique often has incorporated into solution procedure here [8].

- The flow domain is divided into equally spaced segments each of length Δx where,

$$\Delta x = \frac{L}{N - 1} \quad \dots (39)$$

- The conditions at throat section is specified,
 $DR(1)=1.0$, $PR(1)=1.0$, $VR(1)=1.001$, $ER(1)=1.0$ and $ERE=ERE(N)=3.0$ or 4.0 .
- Near the throat (minimum cross-sectional area) the velocity ratio VR is so small that can be assumed as $VR(i) = VR(1)$. This will make density ratio behave as,

$$DR(i) = \frac{DR(1).ER(1)}{ER(i)} \quad \dots (40)$$

- The results of density ratio are used from (2) to (N) points to find the values of pressure ratio of same points according to,

$$PR(i) = PR(1) \left(\frac{DR(i)}{DR(1)} \right)^k \quad \dots (41)$$

- The velocities from (2) to (N) are updated using the first order finite-difference approximation to equation (35).
- The density ratio values are updated using equation (28) by employing under relaxation procedure to get,

$$DR(i) = DR(i) + r \left(\frac{DR(1).VR(1).ER(1)}{VR(i).ER(i)} - DR(i) \right) \quad \dots (42)$$

Then equations (11), (14), (23), (24) and (27) are used to find the remaining flow properties ratios.

- A check is achieved at all points for convergence of solution so that,

$$\frac{|DR(i)_{\text{new}} - DR(i)_{\text{old}}|}{DR(i)_{\text{old}}} < 0.001 \quad \dots (43)$$

The estimation is carried out on Fortran Power Station using finite difference approximation to the space. In the present study air is chosen as the working fluid.

6. NUMERICAL APPROXIMATION FOR ADIABATIC FRICTIONAL FLOW

The effect of friction is usually introduced through momentum conservation [12], as shown in

$$-dF - A \cdot dP = \rho \cdot v \cdot A \cdot dv \quad \dots (44)$$

Frictional force will be found from,

$$-dF = -\frac{\sqrt{\pi} \cdot \bar{f} \cdot \rho \cdot v^2 \cdot A \cdot dx}{\sqrt{A}} \quad \dots (45)$$

Substituting equation (45) into equation (44) and dividing the result by $\rho \cdot v \cdot A \cdot dx$. Since dx represent the difference between any two nodes its value is unity,

$$-\frac{\sqrt{\pi} \cdot \bar{f} \cdot v^2}{\sqrt{A}} - \frac{dP}{\rho} = v dv \quad \dots (46)$$

Changing these values into dimensionless form,

$$-\frac{\sqrt{\pi} \cdot \bar{f} \cdot v^{*2} \cdot VR^2}{\sqrt{A^*} \cdot ER} - \frac{P^* \cdot dPR}{\rho^* \cdot DR} = \frac{v^{*2} \cdot dVR^2}{2} \quad \dots (47)$$

Since,

$$\frac{P^*}{P} = R \cdot T^*, M^2 = 1 = \frac{v^{*2}}{k \cdot R \cdot T^*} \text{ and } A^* = ER(1)$$

$$RT^* = \frac{v^{*2}}{k} = \frac{P^*}{\rho^*} \quad \dots (48)$$

Equation (47) then becomes,

$$-\frac{\sqrt{\pi} \cdot \bar{f} \cdot VR^2}{\sqrt{ER(1) \cdot ER}} - \frac{dPR}{k \cdot DR} = \frac{dVR^2}{2} \quad \dots (49)$$

Carrying out back spacing of the differentials,

$$-\frac{\sqrt{\pi} \cdot \bar{f} \cdot VR(i)^2}{\sqrt{ER(1) \cdot ER(i)}} - \frac{PR(i) - PR(i-1)}{k \cdot DR(i)} = VR(i)(VR(i) - VR(i-1)) \quad \dots (50)$$

Simplifying to the numerical model as,

$$VR(i) = VR(i-1) - \frac{\sqrt{\pi} \cdot \bar{f} \cdot VR(i)}{\sqrt{ER(1) \cdot ER(i)}} - \frac{PR(i) - PR(i-1)}{k \cdot DR(i) \cdot VR(i)} \quad \dots (51)$$

Then the effect of friction on the second term of right hand side in equation (51) and more exactly at average friction factor can be added. The values of average friction factor used in present study is chosen according to references [5], [6] and [9] as well as to experimental results from literature mentioned before in introduction.

Most application values of \bar{f} were restricted between 0.001-0.003 depending on surface roughness as well known. In present study we examine nine values of average friction factors.

7. INTRODUCING OF HEAT TRANSFER AT ISOTHERMAL CONDITION FLOW INTO FRICTIONAL AREA VARIATION FRICTIONAL MODEL FORMULATION

The equation of state is,

$$P = \rho \cdot R \cdot T \quad \dots (52)$$

Its critical state is,

$$P^* = \rho^* \cdot R \cdot T^* \quad \dots (53)$$

The dimensionless form is,

$$PR = DR \cdot TR \quad \dots (54)$$

Since for isothermal flow $TR = 1.0$,

$$PR = DR \quad \dots (55)$$

Dividing (i) state on initial state of equation (55),

$$PR(i) = \left(\frac{PR(1)}{DR(1)} \right) DR(i) \quad \dots (56)$$

Since chocking takes place at $\left(\frac{1}{\sqrt{k}} \right)$, velocity equation becomes,

$$M^2 = \frac{1}{k} = \frac{v^{*2}}{k \cdot R \cdot T^*} \quad \dots (57)$$

Simplifying,

$$R \cdot T^* = v^{*2} \quad \dots (58)$$

The (k) values will be omitted from equations (49), (50) and (51) to be,

$$VR(i) = VR(i-1) - \frac{\sqrt{\pi} \cdot \bar{f} \cdot VR(i)}{\sqrt{ER(1) \cdot ER(i)}} - \frac{PR(i) - PR(i-1)}{DR(i) \cdot VR(i)} \quad \dots (59)$$

The adiabatic law gives us the stagnation temperature ratio,

$$T_o = T \left(1 + \left(\frac{k+1}{2} \right) M^2 \right) \quad \dots (60)$$

The critical form will be,

$$T_o^* = T^* \left(1 + \left(\frac{k+1}{2} \right) \left(\frac{1}{\sqrt{k}} \right)^2 \right) \quad \dots (61)$$

The dimensionless form becomes,

$$TZR = TR \left(\frac{1 + \left(\frac{k-1}{2}\right) M^2}{1 + \frac{k-1}{2\sqrt{k}}} \right) \quad \dots (62)$$

For isothermal condition,

$$TZR = \frac{1 + \left(\frac{k-1}{2}\right) M^2}{1 + \frac{k-1}{2\sqrt{k}}} \quad \dots (63)$$

$$M = \frac{VR(i)}{\sqrt{k}} \quad \dots (64)$$

Entropy change equation becomes,

$$S - S^* = \left(\frac{k \cdot R}{k-1} \right) \ln \left[\frac{T}{T^*} \right] - R \ln \left[\frac{P}{P^*} \right] \quad \dots (65)$$

In dimensionless form,

$$\frac{S - S^*}{R} = \left(\frac{k}{k-1} \right) \ln TR - \ln PR \quad \dots (66)$$

For isothermal flow,

$$\frac{S - S^*}{R} = -\ln PR \quad \dots (67)$$

8. ISOTHERMAL AREA VARIATION FLOW WITHOUT FRICTION MODEL FORMULATION

The pressure ratio equation will be same as equation (56). Velocity ratio equation will be same as equation (34). Only Mach no. equation will be,

$$M = VR(i) \quad \dots (68)$$

Using equation (21),

$$TZR = \frac{1 + \left(\frac{k-1}{2}\right) M^2}{1 + \left(\frac{k-1}{2}\right)} \quad \dots (69)$$

The dimensionless Entropy change will be as equation (67).

9. RESULTS AND DISCUSSION

Extended results are found from the numerical analysis of mixed (isothermal-frictional-area variant) three types of flow with that of every double (isothermal-area variant) type or singular (area variant) type alone. Figures (2, 4, 6, 8, 10, 12, 14 and 16) show the flow properties ratios of pressure, velocity, density, area, stagnation temperature, Mach no., stagnation pressure and Entropy change as function of distance along nozzle length from throat till exit section for an area ratio configuration of 3.0. The difference is clear between each type of flow and a gradual change when the frictional forces are changed in the flow properties, which is too close to the experimental results from [15], as shown in figures (18-a & b). The same flow properties with Entropy change numerical results against nozzle length but with an area ratio configuration of 4.0 (for the same nozzle length as that of 3.0 area ratio means not just an extension) are shown in figures (3, 5, 7, 9, 11, 13, 15 and 17). A gain a clear change for the different flow types at different frictional forces.

As well known the stagnation temperature and pressure as well as Entropy change are constant in non-frictional and non-heat transfer flow as shown in figures (10, 11, 14, 15, 16, and 17).

Samheri,

Frictional and Constant Temperature Heating Control of Air Flow in Diverging Part of Horizontal Nozzles,
Indian Journal of Engineering, 2016, 13(34), 680-697,

The pressure, density ratios and Entropy change in figures (2, 3, 6, 7, 16, and 17) show a clear decrease for all types of flow but in different amount. At the same time velocity, stagnation temperature and pressure ratios and Mach no. in figures (4, 5, 10, 11, 12, 13, 14, and 15) show an increase in all types of flow and in different amount.

A clear drop (difference) in pressure ratio (at exit section for its actual importance) exceed 10% between mixed and double flow type, and exceed 20% between mixed and singular flow type at 3.0 area ratio configuration, see figure (2). These differences at 4.0 area ratio configuration dropped to 6% between mixed and double flow type, and dropped to 13% between mixed and singular flow type, see figure (3). Velocity ratio (at exit section) dropped to 70% between mixed and double flow type and 72% between mixed and singular flow type at 3.0 area ratio configuration figure (4). At 4.0 area ratio configuration the drop becomes 55% and 51%, respectively figure (5). Other differences in flow properties between the three flow types can be followed in different amounts as shown in the figures (6-17).

In supersonic flow the increase of area will increase the velocity, while both the heat transfer (isothermal) and friction tend to decrease the velocity in different amounts. If we look at the differences in properties throughout the nozzle, we will see that area variation was dominant at the first part of the nozzle on both isothermal and frictional forces.

At the second part of the nozzle a reversal action takes place that isothermal and frictional forces become the dominant on area variation causing an inflection point either maximum or minimum depending on behavior of each property. Also it has been noticed that this inclination point is fixed (either minimum or maximum) for all properties at same frictional forces, as shown in table (1).

Table 1 Isothermal-frictional-area variant points of inflection for all properties as function of nozzle length

Area ratio	\bar{f}	Minimum Point % of Diverging Part Length	Maximum Point % of Diverging Part Length
3.0	0.00100	91	70
	0.00125	89	66.3
	0.00150	87	62.6
	0.00175	85	58.8
	0.00200	83	55
	0.00225	81	51.3
	0.00250	79	47.5
	0.00275	77	43.8
	0.00300	75	40
4.0	0.00100	95	75
	0.00125	93.2	71.3
	0.00150	91.3	67.5
	0.00175	89.4	63.8
	0.00200	87.5	60
	0.00225	85.7	56.3
	0.00250	83.8	52.5
	0.00275	81.9	48.8
	0.00300	80	45

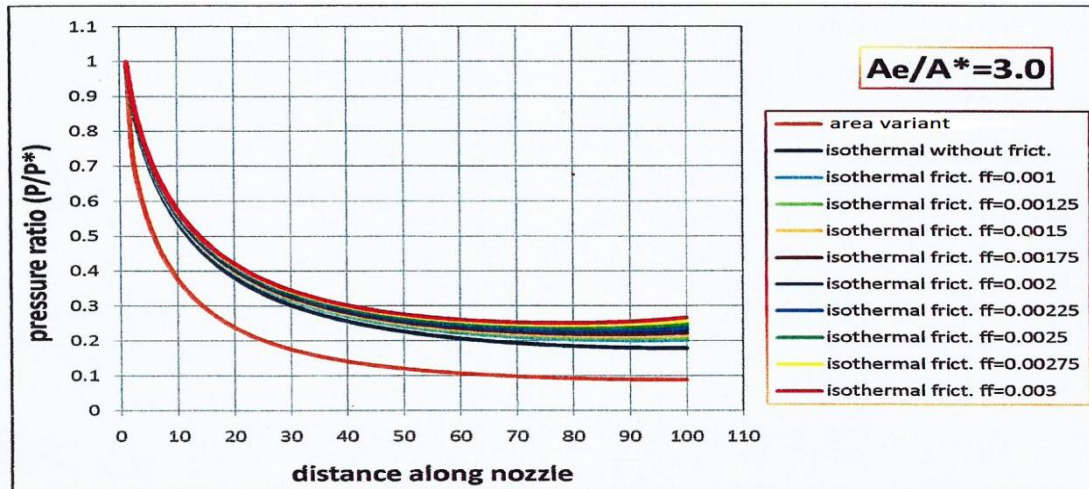


Figure 2 Variation of pressure ratio along nozzle distance for different types of flow at area ratio of 3.0

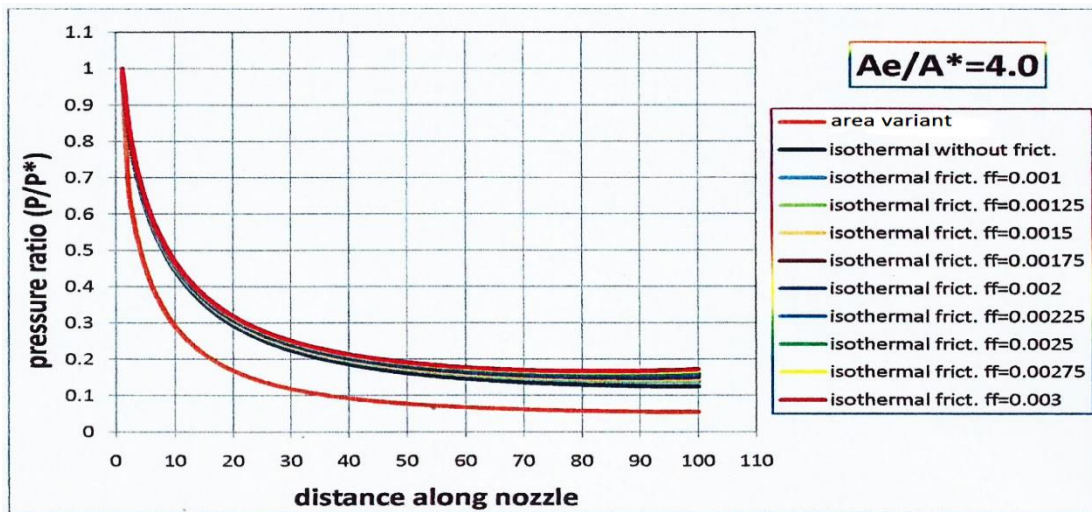


Figure 3 Variation of pressure ratio along nozzle distance for different types of flow at area ratio of 4.0

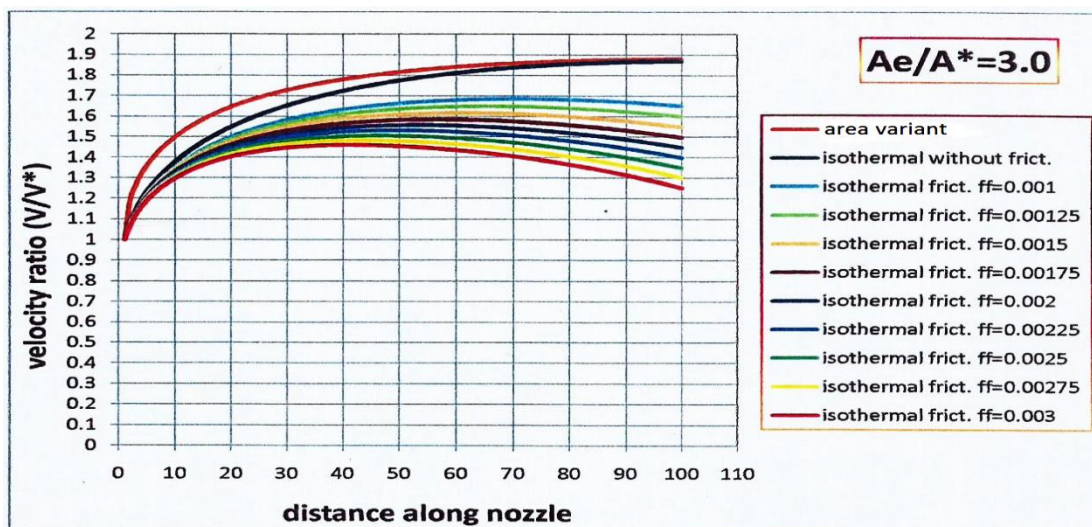


Figure 4 Variation of velocity ratio along nozzle distance for different types of flow at area ratio of 3.0

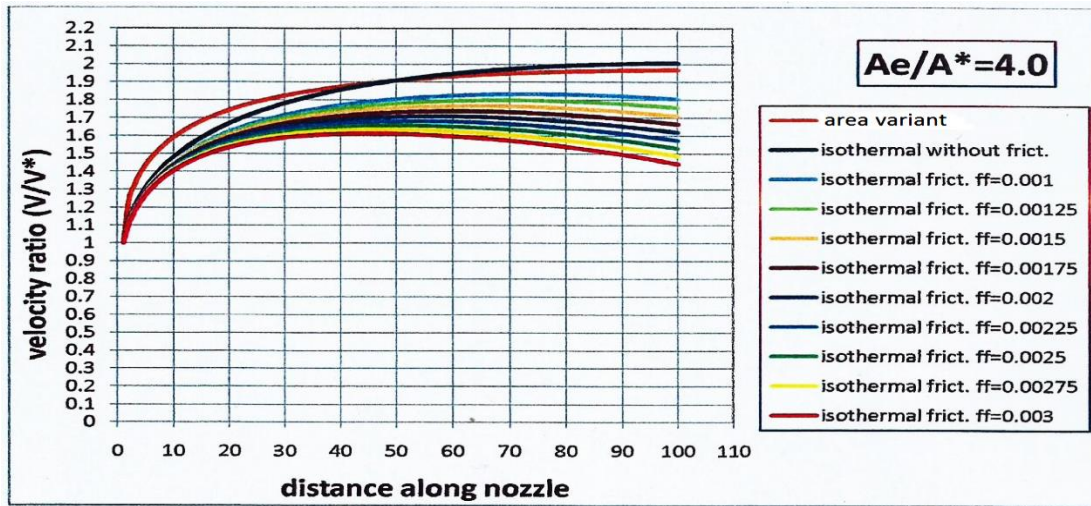


Figure 5 Variation of velocity ratio along nozzle distance for different types of flow at area ratio of 4.0.

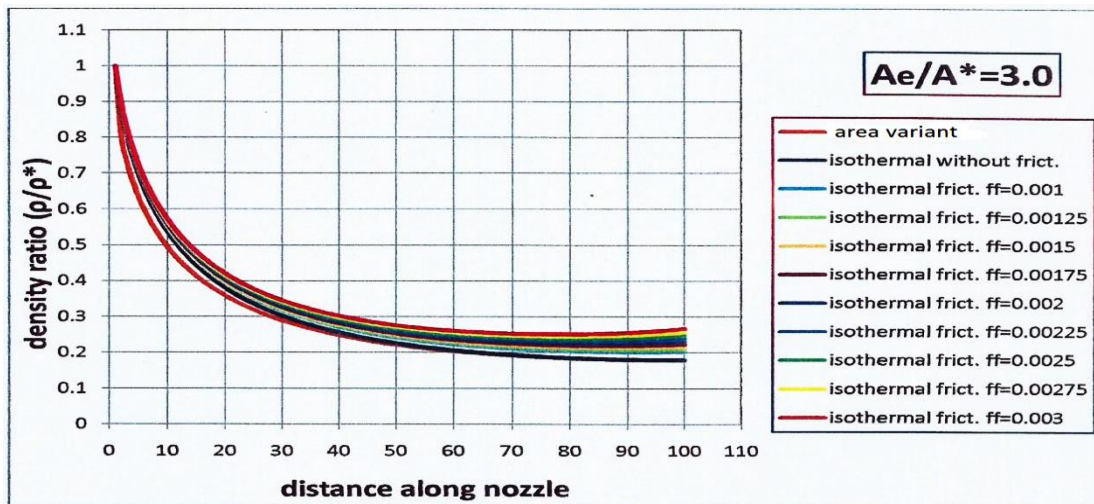


Figure 6 Variation of density ratio along nozzle distance for different types of flow at area ratio of 3.0

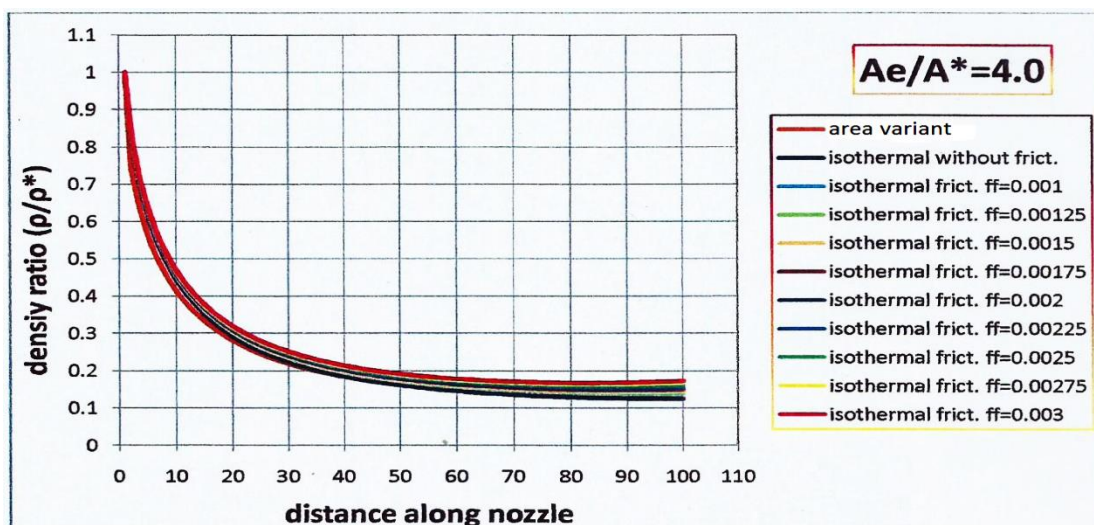


Figure 7 Variation of density ratio along nozzle distance for different types of flow at area ratio of 4.0

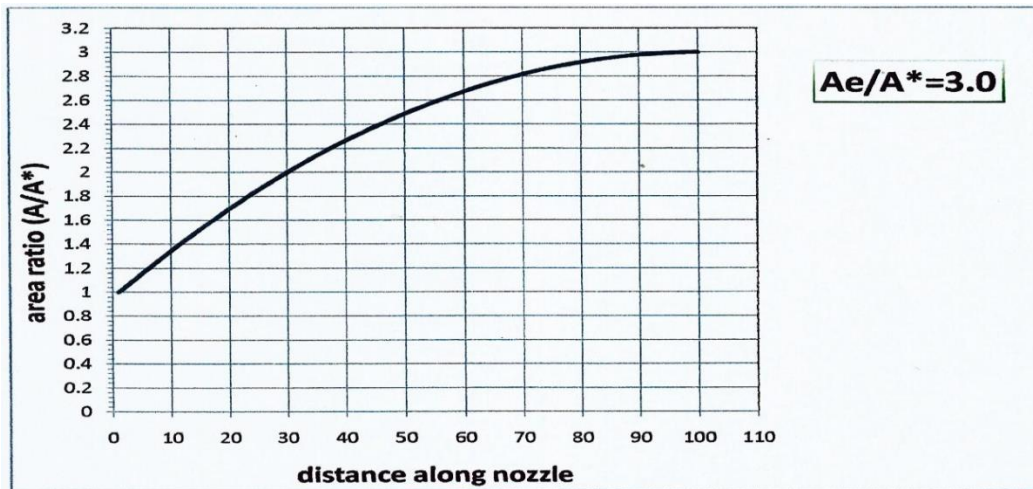


Figure 8 Variation of area ratio along nozzle distance for different types of flow at area ratio of 3.0

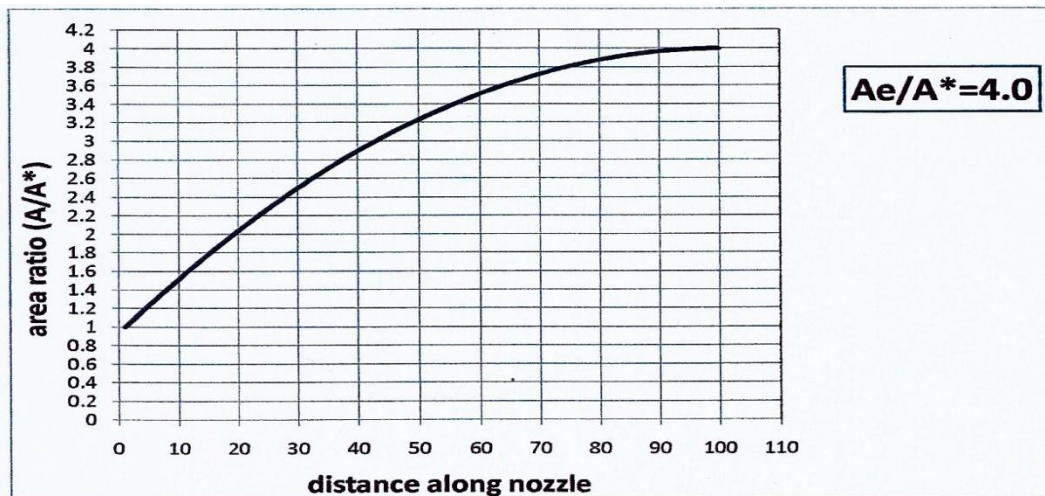


Figure 9 Variation of area ratio along nozzle distance for different types of flow at area ratio of 4.0

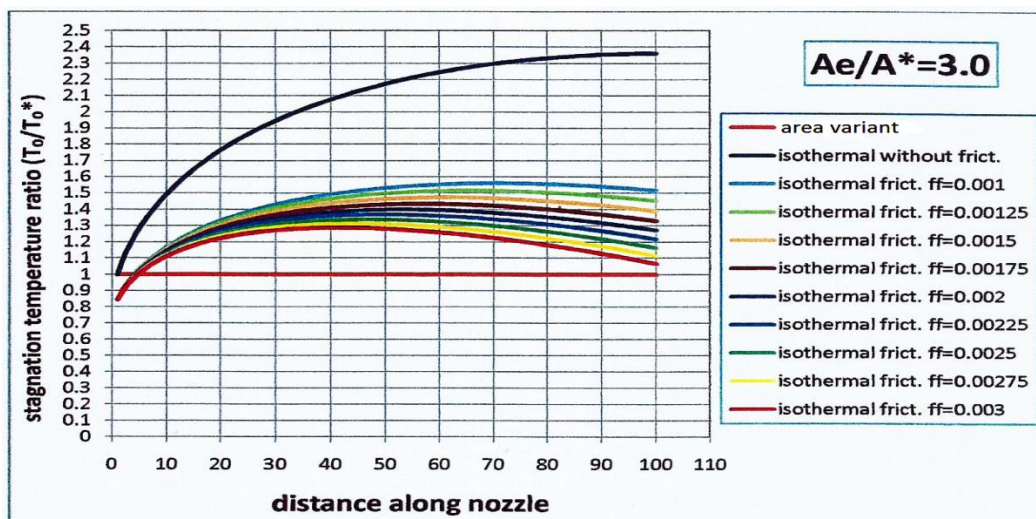


Figure 10 Variation of stagnation temperature ratio along nozzle distance for different types of flow at area ratio of 3.0

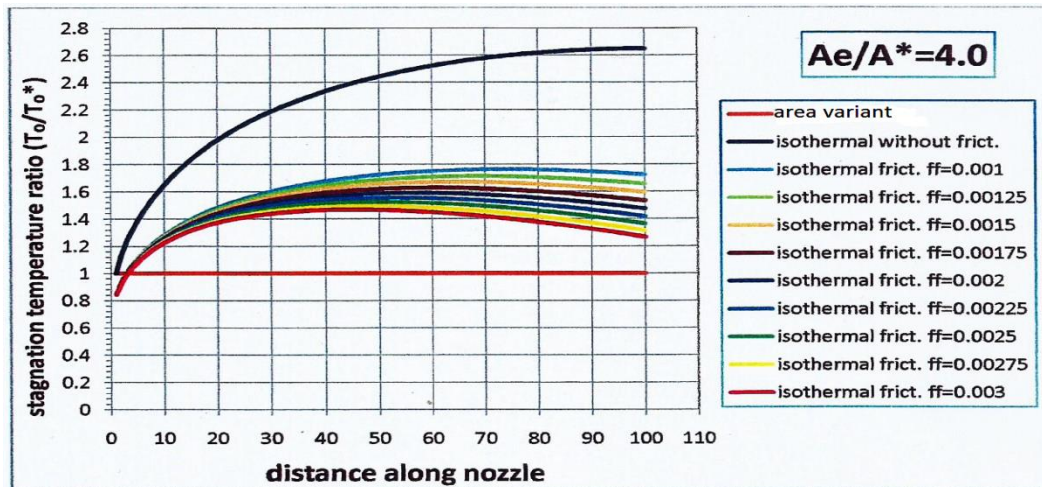


Figure 11 Variation of stagnation temperature ratio along nozzle distance for different types of flow at area ratio of 4.0

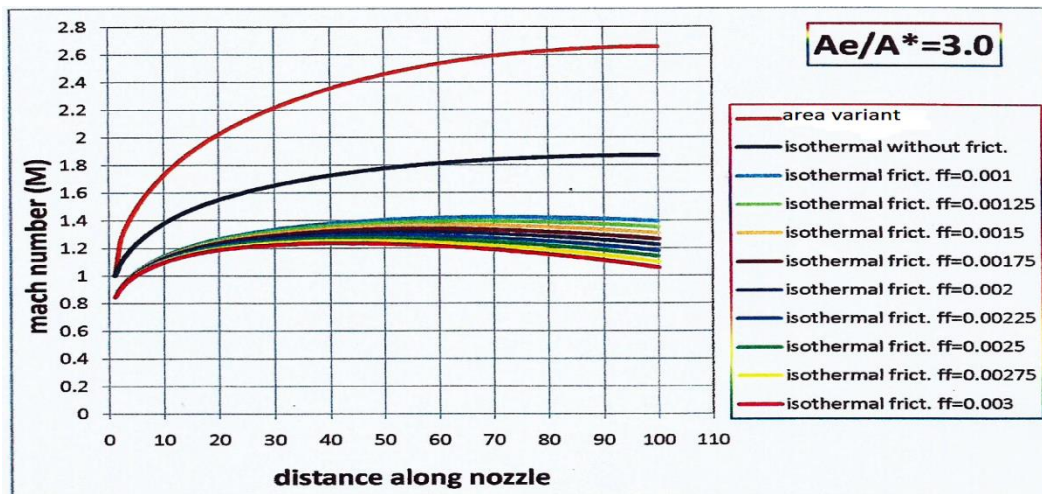


Figure 12 Variation of Mach no. along nozzle distance for different types of flow at area ratio of 3.0

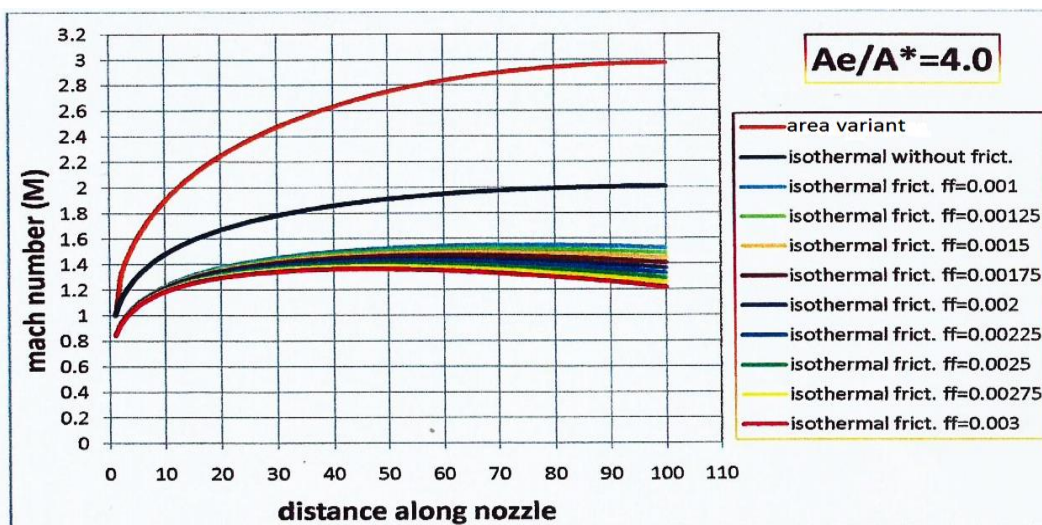


Figure 13 Variation of Mach no. along nozzle distance for different types of flow at area ratio of 4.0

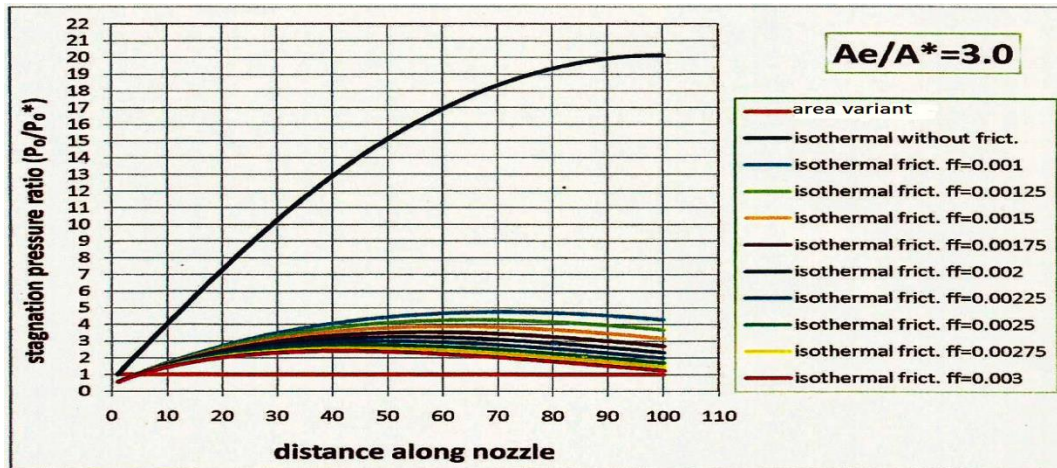


Figure 14 Variation of stagnation pressure ratio along nozzle distance for different types of flow at area ratio of 3.0

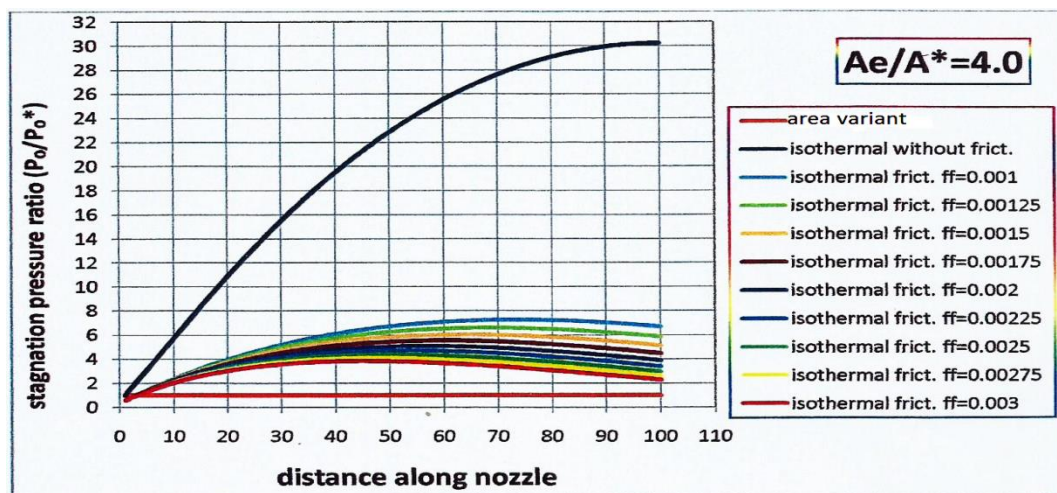


Figure 15 Variation of stagnation pressure ratio along nozzle distance for different types of flow at area ratio of 4.0

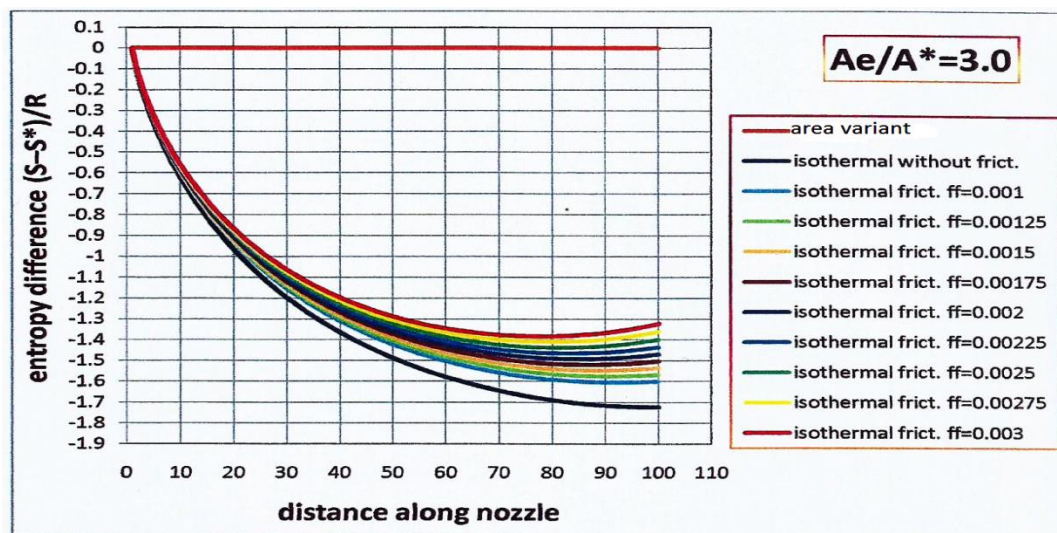


Figure 16 Variation of Entropy change along nozzle distance for different types of flow at area ratio of 3.0

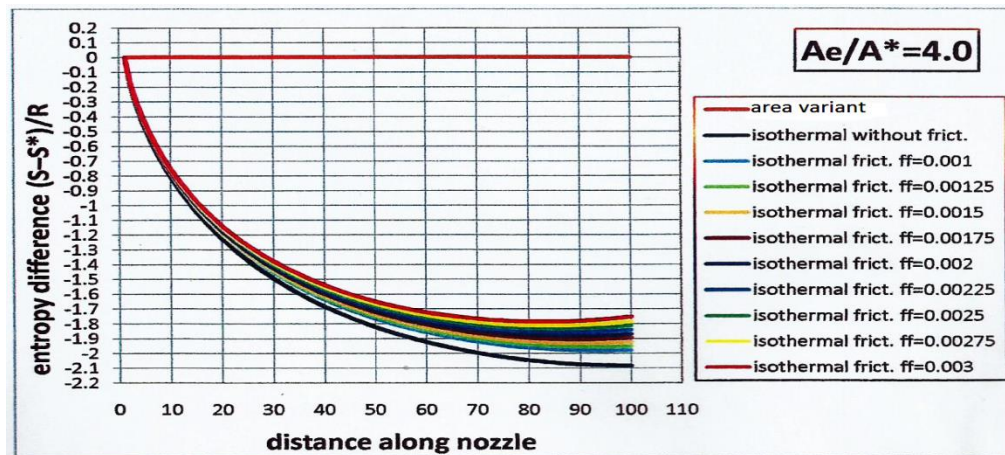


Figure 17 Variation of Entropy change along nozzle distance for different types of flow at area ratio of 4.0

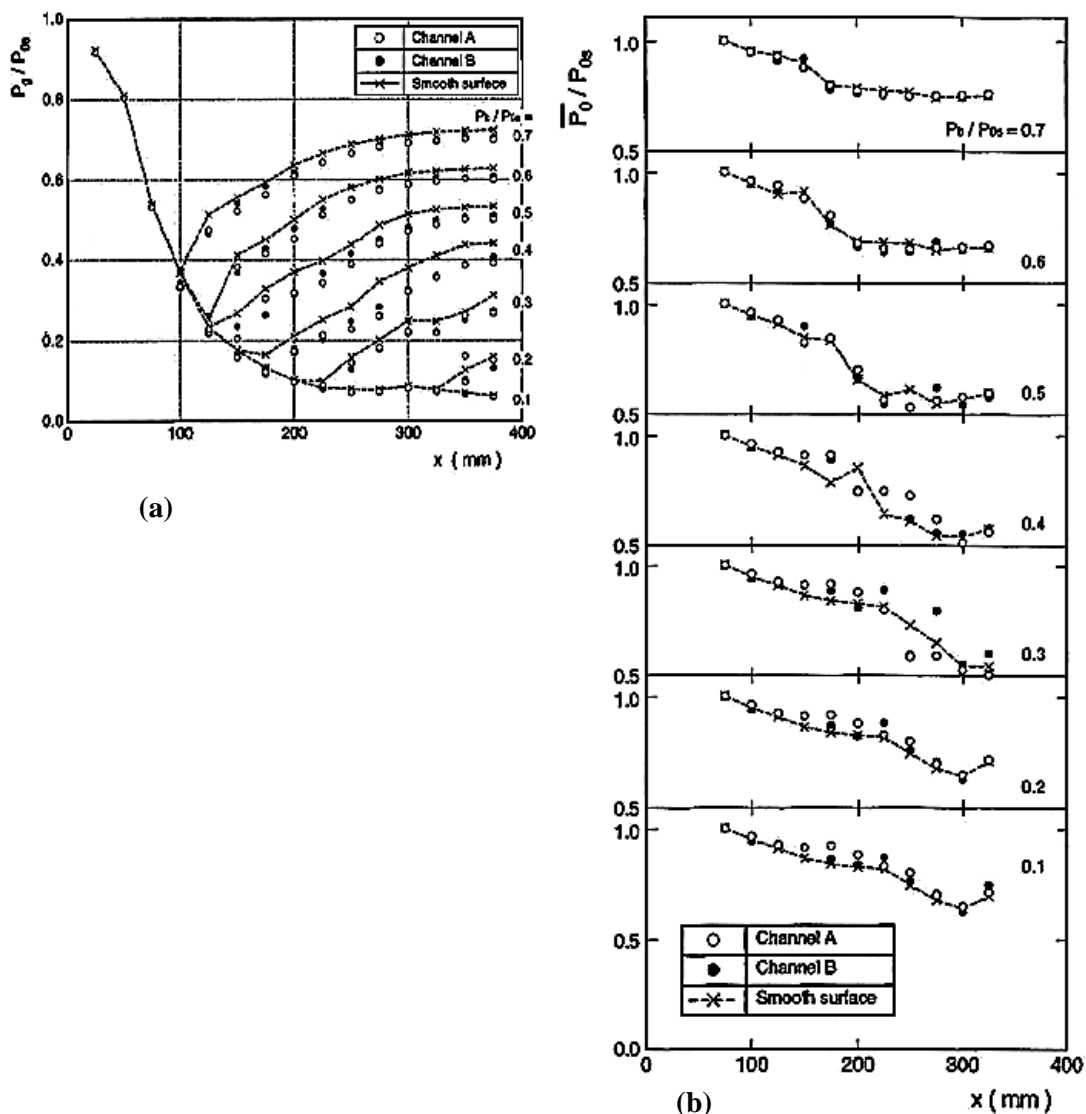


Figure 18 (a) Experimental variation of static pressure ratio along nozzle distance, where 0.2-0.7 present subsonic back pressure ratios and 0.1 present supersonic back pressure ratio [15], (b) Experimental variation of stagnation pressure ratio along nozzle distance [15].

Samheri,
Frictional and Constant Temperature Heating Control of Air Flow in Diverging Part of Horizontal Nozzles,
Indian Journal of Engineering, 2016, 13(34), 680-697,

10. CONCLUSION

The paper studied the full effect of friction at different degrees at the same time with heat transfer under isothermal condition in addition to area variation (mixed type flow) in non-linear curvatures. The bigger difference in flow properties is graduated from pressure, Entropy change, Mach no., stagnation temperature, velocity, stagnation pressure and density ratios, respectively. The numerical analysis gives a clear shift between the variables in the three types of flow (mixed, double and singular) and good agreement with the found experimental results. The new behavior of frictional-isothermal-area variant flow show a concave or convex shapes of variable changes, which are not known before either in double or singular flow types.

AKNOWLEDGMENT

The author is grateful to Prof. Dr. Adnan A. Rasool the head of Department of mechanical Engineering, Al-Mustansiriyah University, Baghdad, Iraq as well as Asst. Prof. Dr. Dhirgham A.H. Al-khafaji, Department of mechanical Engineering, Babylon University, Babylon, Iraq and Prof. Dr. Rafid Alghadar Liverpool John Moores University, Liverpool, UK for all support and assistance.

REFERENCES

1. Aksel M.H., and Erlap O.C., "Gas Dynamics", Prentice Hall International (UK) Ltd, 1994.
2. Al-Kafaji W., and Tooley J.R., "Numerical Methods in Engineering Practice", HRW International Edition, CBS College Publishing, 383 Madison Avenue, New York, NY 10017, 1986.
3. Anderson J.D., Jr., "Modern Compressible Flow with Historical Perspective" 2nd edn. McGraw-Hill, New York, 1990.
4. Bandyopadhyay A. and Majumdar A., "Modeling of Compressible Flow with Friction and Heat transfer using the Generalized Fluid System Simulation Program (GFSSP)", *Thermal and Fluid Analysis Workshop (TFAWS)* to be hosted by NASA Glenn Research Center and Corporate College, Cleveland, Sep. 10-14, 2007.
5. Brower W.B., "Theory, Tables, and Data for Compressible Flow", Hemisphere, New York, 1990.
6. Churchill S.W., "Friction Factor Equation Spans All Fluid Flow Regimes", *Chemical Engineering*, 91-2, 7 Nov. 1977.
7. Emanuel G., "Gas dynamics: Theory and Application", AIAA, Washington, 1986.
8. Hodge B.K., and Koenig K., "Compressible Fluid Dynamics with Personal Computer Applications", Prentice Hall, Englewood Cliffs, NJ, 1995.
9. Keenan, J.H. and Neumann, E.P., "Measurements of Friction in a Pipe for Subsonic and Supersonic Flow of Air", *Journal of Applied Mechanics* 13(2), A-91, 1946.
10. Kutler P., Warming R.F. and Lomax H., "Computation of Space Shuttle Flow Fields using Noncentered Finite-Difference Schemes", *AIAA Journal* 11(2), 196-204, 1973.
11. Oosthuizen P.H., and Carscallen W.E., "Compressible Fluid Flow", McGraw-Hill Companies, Inc, 1997.
12. Pai S., and Luo S., "Theoretical and Computational Dynamics of a Compressible Flow", Van Nostrand Reinhold, New York, 1991.
13. Saad M.A., "Compressible Fluid Flow", 2nd edn. Prentice Hall, Englewood Cliffs, NJ, 1992.
14. Warsi Z.U.A., "Fluid Dynamics-Theoretical and Computational Approaches, CRC Press, Boca Raton, FL, 1993.
15. Tsunoda K., Suzuki T., and Asai T., "Improvement of the Performance of a supersonic Nozzle by Riblets", *Transactions of ASME, Journal of Fluids Engineering*, Vol.122, PP. 585-591, Sep. 2000.
16. Yahya S.M., "Fundamentals of Compressible Flow", Wiley Eastern, New Delhi, 1982.
17. Young F.M., "Generalized One-dimensional, Steady Compressible Flow", *AIAA Journal* 31(1), 204-8, 1993.